

A Molecular-Dynamics Simulation of Hydrogen-Induced Amorphization

Masahiko Katagiri and Hidehiro Onodera

National Research Institute for Metals, 1-2-1 Sengen, Tsukuba, Ibaraki 305-0047, Japan

Fax: +81-(0)298-59-2601, e-mail: katagiri@nrim.go.jp

The hydrogen-induced amorphization (HIA) of C15 Laves phase was studied. We discuss HIA from Bulk modulus and Molecular Dynamics (MD) results. It is shown that the HIA temperature is correlated with Bulk modulus and amorphization occurs at lower temperature in softer materials. HIA occurs if a certain amount of hydrogen is added to the crystal. MD results show that the distance among Lanthanoid atoms increases and that among transition metal atoms decrease due to HIA. The incorporation of hydrogen imposes the local stress in the crystal and destructs the crystal structure.

Key words: Molecular Dynamics, Hydrogen Induced Amorphization, Embedded Atom Method, C15, Laves, CeNi₂

1. INTRODUCTION

The microstructure control of the transition process from amorphous state to crystalline one is a possible method to improve performance of various metallic materials by microstructure refinement. Recently Aoki et al. [1] have observed the formation of amorphous metallic alloys by the hydrogenation of the AB₂ Laves phases (A = rare earth, B = Fe, Co, Ni), called *hydrogen-induced amorphization* (HIA). In view of industrial applications, the HIA is one of probable methods to prepare amorphous alloys since the hydrogenation and dehydrogenation can be done easily and rapidly without any traces in materials. For the effective utilization of HIA to the microstructural control, it is necessary to reveal the mechanism of HIA. Thus, the goal of the present study is to understand the microscopic mechanism of the HIA by using molecular dynamics simulations.

Recent development in semi-empirical techniques describing many body interactions in computer simulations has been successfully applied to phenomena in metals. To simulate HIA, it is necessary to treat systems of large size. Moreover, many-body effects may play an important role in metals. Therefore, semi-empirical technique is powerful in this area. We describe the atomic interaction by the embedded-atom method (EAM).

2. METHOD

The EAM that was originally developed by Daw and Baskes was first applied to hydrogen embrittlement in metals [2]. EAM is one of the so-called *glue models*. The physical picture is of ions embedded in an electron sea, which act like glue to hold them together. Daw and Baskes proposed the following expression of the energy [3],

$$E = \sum_i F^i(\rho^i) + \frac{1}{2} \sum_{i,j(j \neq i)} \phi^{ij}(r^{ij}) \quad (1)$$

Here $F^i(\rho^i)$ is the embedding energy of atom i , ρ^i is the background electron density in the host matrix at the position r^{ij} in the absence of atom i . The atom i experiences a locally uniform electron density. $\phi^{ij}(r^{ij})$ is the short-range pairwise ionic-core repulsion. At this level of approximation, the embedding energy functional in a host matrix is identical to that in jellium. We make a further simplification by assuming that the host charge density is approximated by a linear superposition of the atomic densities of the host atom.

$$\rho^i = \sum_{j(j \neq i)} \rho_a^j(r^{ij}) \quad (2)$$

By this approximation, it is not necessary to solve for the self-consistent density. The force f^i on atom i is determined by,

$$f^i = - \sum_{j(j \neq i)} \left[\frac{\partial F^i}{\partial \rho^i} \frac{\partial \rho^j}{\partial r^{ij}} + \frac{\partial F^j}{\partial \rho^j} \frac{\partial \rho^i}{\partial r^{ij}} + \frac{\partial \phi^{ij}}{\partial r^{ij}} \right] \hat{r}^{ij} \quad (3)$$

The EAM parameters for Ce and Ni were obtained by Johnson-Oh method [4]. In this method, electron density and short-range pair potential have the forms,

$$\rho(r) = \rho_0 \exp\{-\beta(r/r_0 - 1)\} \quad (4)$$

$$\phi(r) = \phi_0 \exp\{-\gamma(r/r_0 - 1)\} \quad (5)$$

r_0 is the equilibrium interatomic separation distance.

The valence electron density of an atom was calculated by fully relativistic all-electron density functional method (BDF) [5]. The density by BDF decays more rapidly than that by Non-relativistic

Hartree-Fock-Slater calculation (Herman-Skillman) named CAEL [6]. It was fitted to the exponential form. Table I shows the range of fitting and the result. Experimental values used in parameterization are listed in Table II [7, 4, 8, 9, 10]. The EAM potential for H were taken from Ref. [3].

Table I The lower and upper cutoff radii r_{lc} and r_{uc} are shown. The valence electron densities were fitted by the exponential form. The length is in Å and the density is in 10^{14}Å^{-3} .

	R_0	R_{lc}	r_{uc}	ρ_0	β
Ni	2.49	2.0	5.0	5.38 ⁴	7.14
Ce	3.65	2.0	6.0	1.82 ⁴	7.62

Table II Experimental data of cohesive energy (E_c), vacancy formation energy (E_{lv}^f), Bulk and Shear modulus B and G. E_c is in eV and B and G are in 10^{12}erg/cm^3 .

	E_c	E_{lv}^f	B	G
Ni	4.45	1.6	1.804	0.947
γ -Ce	4.32	0.72	0.215	0.135

The unit cell length for the MD simulations is 14.4Å with 64 Ce and 128 Ni atoms. H atoms are added to the crystal while controlling the instantaneous temperature at 300K, using the Heat-Bath contact method [11]. 100,000 MD steps were used to equilibrate, and successive 50,000 steps were used for sampling. The time interval is 0.1 fsec.

3. RESULTS AND DISCUSSION

3.1 Phenomenological Viewpoint

Table III shows the ratio of the atomic radii R_A/R_{Co} , where R_A is radius of Lanthanoid atom and R_{Co} is that of Co atom in *pure* crystal [12]. AB_2 C15 Laves phase is so called *size factor compound* and the ideal ratio is $R_A/R_B = 1.225$ [1]. The radii of A and B atoms are adjusted to satisfy this ratio in Laves phase.

Table III The ratio R_A/R_{Co} is shown. R_A and R_{Co} are atomic radii of Lanthanoides and Co atom in pure crystals, respectively.

La	Ce	Pr	Nd	Pm
1.504	1.464	1.464	1.456	1.440

Sm	Eu	Gd	Tb	Dy
1.432	1.592	1.424	1.408	1.400

Ho	Er	Tm	Yb	Lu
1.400	1.392	1.408	1.552	1.384

Figure 1 shows HIA temperature T_a of ACo_2 [13]. It is known that the larger R_A/R_{Co} gives smaller T_a . As Aoki et al. Pointed out [1], one can arrange HIA by atomic size ratio R_A/R_B . We found the existence of correlation between Bulk modulus B_{AB2} and T_a . Figure 2 shows B_{ACo2} calculated from those of *pure* crystals B_A and B_{Co} by simple combination rule (see Appendix A),

$$B_{ACo2} = 0.479B_A + 0.521B_{Co} \quad (6)$$

The data of pure systems were taken from Ref. [9]. Phenomenologically, the softer material gives lower HIA temperature as Chung et al. [14] proposed. This is also true in AFe_2 and ANi_2 cases. The predicted Bulk moduli of AFe_2 and ANi_2 are similar to that of ACo_2 . The larger R_A/R_B gives smaller Bulk modulus and lower T_a . Experimentally, the amorphization occurs at about 173K in $CeNi_2$, while it does above 450K in $ErNi_2$. This difference can be explained by the difference of Bulk modulus. $CeNi_2$ is softer than $ErNi_2$.

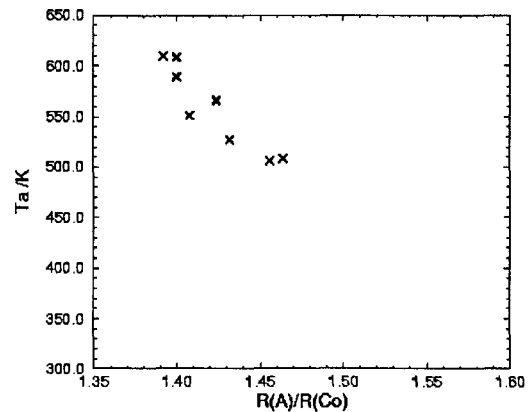


Fig.1 HIA temperature of ACo_2 is shown.

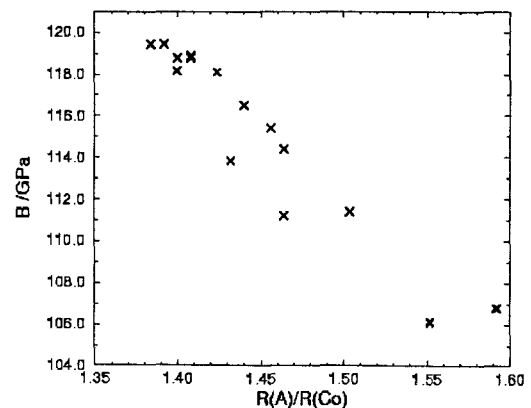
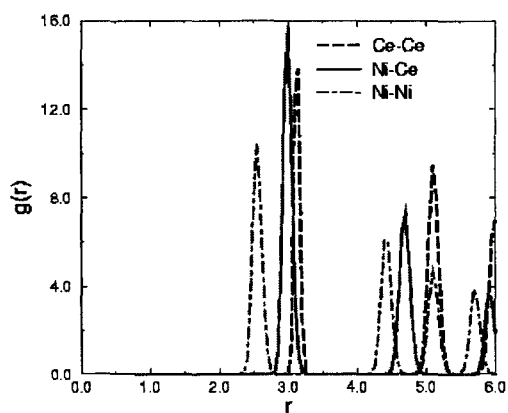


Fig.2 Bulk moduli of ACo_2 C15 Laves phase calculated by combination rule are shown.

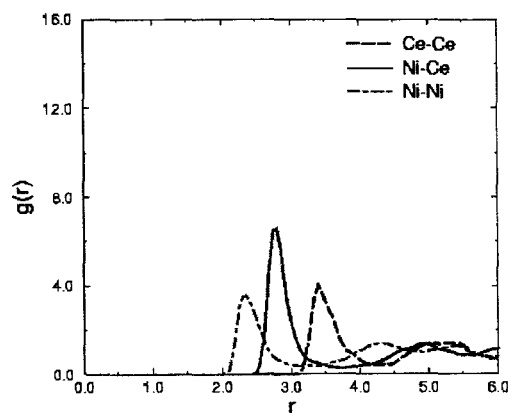
3.2 Molecular Dynamics

We simulated HIA in CeNi_2 system at 300K. We found that HIA takes place in CeNi_2H_3 at 300K. However, if the amount of H is less than 25%, i.e. CeNi_2H , it does not occur. Without H, amorphization does not occur. The initial process of amorphization seems to destroy the crystal structure mechanically. Moreover, HIA takes place within a few lattice vibration periods. This means that the HIA does not require the thermally activated diffusion kinetics. This is why the HIA in CeNi_2 takes place at very low temperature compared to the melting point T_m ($T_m = 830\text{K}$).

Figure 3 shows the radial distribution functions $g(r)$ between Ce and Ni for (a) crystal- CeNi_2 and (b) amorphous- CeNi_2H_3 at 300K. The first neighbor shell of Ce-Ce and Ni-Ni becomes expanded and compressed respectively by HIA. Note that in Laves phase, Ce and Ni are compressed and expanded, respectively. By HIA, these compression and expansion are relaxed. This agrees with experiment [13, 1].



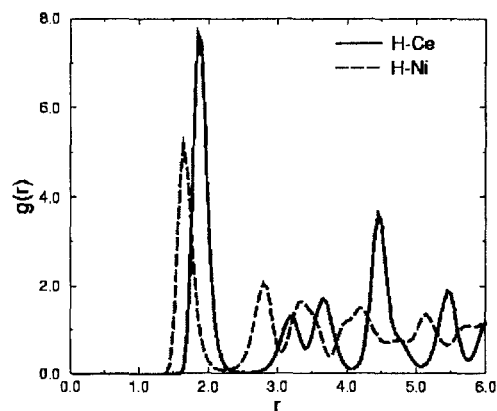
(a) crystal- CeNi_2 at 300K



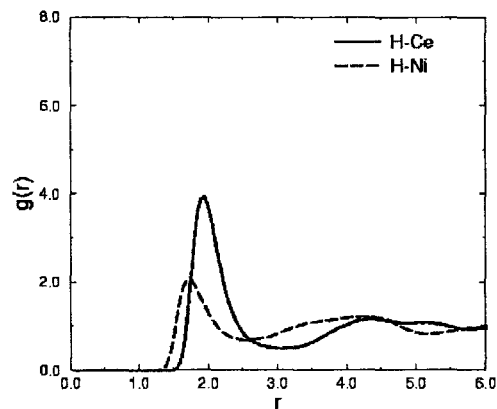
(b) amorphous- CeNi_2H_3 at 300K

Fig.3 Radial distribution functions in (a) crystal- CeNi_2 and (b) amorphous- CeNi_2H_3 at 300K are shown. r is interatomic distance in Å.

Figure 4 shows $g(r)$ between H and Ce and Ni for (a) crystal phase at 100K and (b) amorphous phase at 300K in CeNi_2H_3 . By HIA, the ratio of the first peak $g(\text{H-Ce})/g(\text{H-Ni})$ increases from about 1.5 to 2.0. It is known that in crystal phase H exists in the tetrahedral sites, i.e., $2\text{Ce}+2\text{Ni}$ and $1\text{Ce}+3\text{Ni}$ sites. In amorphous phase H can exist in 4Ce , $3\text{Ce}+1\text{Ni}$, $2\text{Ce}+2\text{Ni}$ and $1\text{Ce}+3\text{Ni}$ sites. H can hold more Ce atoms in the first neighbor shell by amorphization.



(a) crystal- CeNi_2H_3 at 100K



(b) amorphous- CeNi_2H_3 at 300K

Fig.4 Radial distribution functions in (a) crystal- CeNi_2H_3 at 100K and (b) amorphous- CeNi_2H_3 at 300K between H and Ce or Ni are shown. r is interatomic distance in Å.

The first peak of $g(\text{H-Ce})$ is outer than $g(\text{H-Ni})$. There exists stronger H-Ce repulsion than H-Ni one. In tetrahedral sites, thus H exists in the position closer to Ni than Ce. In Laves phase, Ce atom is compressed and, thus, is in repulsive region. The incorporation of H imposes H-Ce repulsion (or local stress) and leads to the destruction of the structure. The softening of the

material by H incorporation, which appears in the change of Bulk modulus, helps this destruction. After HIA, H-Ce distance becomes larger as a result of relaxation of repulsion as shown in the H-Ce first peak in Fig.4. We also found that the main HIA process is the movement of Ni rather than Ce.

The many-body effects may also be important in HIA. From viewpoint of pair potential, highly symmetric structures are stabilized and the configuration energy is the lowest in the perfect crystal. The many body effects play an important role when the local environment of an atom is of sufficiently low symmetry or has low coordination number. The low coordination decreases the repulsive three-body contribution. The activation energy for HIA is lowered by the presence of many-body effects, because this stabilizes the low symmetry.

4. CONCLUSIONS

The hydrogen-induced amorphization (HIA) was simulated by molecular dynamics using embedded-atom method, especially for CeNi₂ C15 Laves phase. We found that HIA takes place in CeNi₂ H₃ at 300K. However, if the amount of H is less than 25%, i.e. CeNi₂H, it does not occur. Without H, amorphization does not occur. The incorporation of H imposes the local stress in the crystal and destroys the structure mechanically. The relaxation takes place to decrease the repulsion. Amorphization occurs easily in the softer materials, which is revealed in the Bulk modulus. It was observed that the movement of Ni is the main process of amorphization. In the final amorphous structure, H tends to exist in Ce cage, rather than Ni cage.

ACKNOWLEDGEMENTS

The authors are grateful to Dr. W. Liu for help in use of BDF and helpful comments. We also thank Drs. M. Shimono and T. Sasaki at NRIM for helpful discussion.

Appendix A combination rule of Bulk modulus

Here we give the combination rule of the bulk modulus of C15 Laves phase. The total volume V per formula unit is the summation of the Wigner-Seitz cell volumes V_A and V_B .

$$V = V_A + 2V_B \quad (A1)$$

The ratio of V_B and V_A is constant in the volume change, i.e.,

$$\xi = \frac{V_B}{V_A} = \text{const.} \quad (A2)$$

The total energy per formula unit can be written as,

$$E = E_A + 2E_B. \quad (A3)$$

By taking second derivative, we get the Bulk modulus B_{AB2} .

$$B_{AB2} = V \frac{d^2 E}{dV^2} = \frac{1}{1+2\xi} B_A + \frac{2\xi}{1+2\xi} B_B \quad (A4)$$

Since the radii of A and B atoms are calculated from the lattice parameters by,

$$\begin{aligned} r_A &= \sqrt{3}a/8 \\ r_B &= \sqrt{2}a/8 \end{aligned} \quad (A5)$$

Then we get combination rule,

$$B_{AB2} = 0.479B_A + 0.521B_B \quad (A6)$$

with the atomic partial bulk moduli

$$B_{A,B} = V_{A,B} \frac{d^2 E_{A,B}}{dV_{A,B}^2}. \quad (A7)$$

One can get the arithmetic mean of the bulk moduli by setting $\xi = 1$.

References

1. I. K. Aoki, X. G. Li, and T. Masumoto, *Acta Metall. Mater.* **40**, 1717 (1992).
2. M. S. Daw and M. I. Baskes, *Phys. Rev. Lett.* **50**, 1285 (1983).
3. M. S. Daw and M. I. Baskes, *Phys. Rev. B* **29**, 6443 (1984).
4. D. J. Oh and R. A. Johnson, *J. Mater. Res.* **3**, 471 (1988).
5. W. Liu and M. Dolg, *Phys. Rev. A* **57**, 1721 (1998).
6. J. C. A. Boeyens, *J. Chem. Soc. Faraday Trans.* **90**, 3377 (1994).
7. S. M. Foiles, M. I. Baskes, and M. S. Daw, *Phys. Rev. B* **33**, 7983 (1986).
8. M. Boidron and R. Paulin, *Phys. Lett. A* **73A**, 200 (1979).
9. C. Kittel, *Introduction to solid state physics*, 6th ed. (John Willey & Sons, Inc., New York, U.S.A., 1986).
10. D. R. Lide, *CRC handbook of Chemistry and Physics*, 79th ed. (CRC Press, Washington, D.C., 1998).
11. M. Katagiri, M. Kubo, and A. Miyamoto, *Shokubai* **36**, 50 (1994).
12. *Kinzoku Data Book*, 3rd ed. (Maruzen, Tokyo, 1993), in Japanese.
13. K. Aoki and K. Masumoto, *Materia Japan* **34**, 126 (1995), in Japanese, and references therein.
14. U. I. Chung, Y. G. Kim and J. Y. Lee, *Philos. Mag. B* **63**, 1119 (1991).